Concentration Dependence of Shear-Induced Polymer Migration in DNA Solutions near a Surface

Lin Fang† and Ronald G. Larson*

Department of Chemical Engineering, University of Michigan, Ann Arbor, Michigan 48109

Received November 16, 2006; Revised Manuscript Received August 15, 2007

ABSTRACT: We investigate optically the time-dependent concentration and mean fractional stretch of λ-phage DNA molecules near a solid surface in a torsional shear flow, for solutions of DNA concentrations from $0.1c^*$ to $3.0c^*$. At high Weissenberg number ($Wi \geq 10$), the polymer migration caused by the hydrodynamic interaction with the surface diminishes as DNA concentration increases from $0.1c^*$ to $1.0c^*$, indicating that screening of wall hydrodynamics occurs to some degree in the concentration range traditionally recognized as "dilute". In addition, the surface migration continues to exist in diminished form up to $3.0c^*$, implying that, while the chains are overlapping, they do not screen out the hydrodynamic interactions completely. On the time scale over which migration occurs, the apparent mean fractional stretch of DNA molecules decreases near the surface, which is probably caused by the selective retention of fragments near the surface as long chains migrate away.

Introduction

On the basis of molecular weight and concentration, polymer solutions have been classified into five different regimes: dilute, semidilute unentangled, semidilute entangled, concentrated unentangled, and concentrated entangled.[1] While Zimm scaling is valid in the dilute limit,[2−5] as has been confirmed by experiments[3,6,7] and computer simulations,[8−10] theoretical understanding is less developed at finite concentrations.[11−20] The concentration regimes somewhat above dilute are affected by the concentration dependence of excluded-volume interactions, hydrodynamic interactions (HI), and entanglements. For solutions concentrated enough that both excluded volume and HI effects are fully screened, but still below the entanglement threshold, the Rouse model has been utilized, while the Doi−Edwards model applies to concentrated entangled solutions and melts.[5,21,22] However, the details of the crossover, the underlying mechanism of the screening of HI, and the concentration dependence of the screening have been subjects of considerable interest and are not yet fully resolved.

Semidilute polymer solutions by definition have polymer concentrations above the minimum value for coil overlap, c^*.[23] Polymer conformations in semidilute solution are well understood in terms of the "blob size" ξ_s,[2] which is a renormalized monomer size. At concentrations above c^*, the polymer behavior changes from Zimm-like to Rouse-like and the "blob size" drops below the radius R_g of the whole polymer coil. This transition can be ascribed to the onset of overlapping of the chains and the subsequent screening of excluded volume interactions and hydrodynamic effects. For long enough chains, increasing further the concentration until it exceeds the critical concentration for entanglement, c_e, causes entanglement effects to begin to dominate the dynamic behavior of macromolecules. To date, it is not entirely clear whether the overlapping chains obey a Rouse-like behavior over the regime $c^* < c < c_e$ or whether in this regime there is instead a slow transition from dilute to entangled behavior.

Using molecular dynamics simulations, Kaznessis et al.[24] found that hydrodynamic and excluded volume effects are effectively screened for *cis*-polyisoprene solutions at concentrations $c > 8c^*$, which conforms well to the dielectric spectroscopy experiments of these solutions. Ng and Leal[25] examined flow birefringence and flow modification effects for two-dimensional extensional flows of polystyrene solutions and found that polymer chain extension is inhibited by intermolecular interactions as the concentration is increased above $0.33c^*$. Significant concentration effects on bulk shear and extensional rheology of DNA solutions are observed at concentrations as low as $0.1c^*$ in Brownian dynamics simulations by Stoltz et al.[26] Ahlrichs et al.[19] used simulations to show that the screening of HI in semidilute is not described correctly unless both the distance and time dependence of HI are accounted for.

Of interest here is the effect of the crossover from dilute to semidilute concentration on polymer HI in the presence of a nearby surface, which is much less studied than is the crossover in the bulk. Among the few available studies, Ausserré et al.[27] investigated optically the thickness of the depletion layer for rodlike xanthan aqueous solutions near a fused-silica wall and found that the depletion layer thickness remains constant until the overlap concentration is reached and thereafter decreases with increasing polymer concentration. Using phenomenological two-fluid models, Chauveteau et al.[28] and Omari et al.[29] found that above the overlap concentration the thickness of the depletion layer diminishes with increasing concentrations of flexible polymer. Very recently, sophisticated Brownian dynamics simulations with full wall-influenced hydrodynamics by Hernández-Ortiz et al.[30] have shown that the shear-thickened wall depletion layer found in dilute solutions, resulting from hydrodynamic interactions with the wall, begins to thin above $0.1c^*$, the same concentration above which bulk hydrodynamic interactions also begin to become screened.

To investigate experimentally in detail the concentration effects on the migration of polymer molecules near a single solid surface, in this article, we perform experiments with λ-phage DNA solutions with concentrations ranging from dilute to semidilute. We measure the time-dependent mean fractional stretch and concentration of stained DNA molecules at a distance of 3 μm away from the stationary surface in a torsional shear flow, where we earlier showed[31] that hydrodynamic interactions

* Corresponding author. E-mail: rlarson@umich.edu.
† Current address: DuPont China Research and Development Center, Zhangjiang Hi-Tech Park, Shanghai, 201203, People's Republic of China.

10.1021/ma0626315 CCC: $37.00
Published on Web 10/12/2007

between the polymer and the surface are strong in very dilute solutions of the same DNA molecules, consistent with other earlier experimental and theoretical work.[32−36]

Experimental Section

Materials. We define c^* as the concentration at which a random equilibrium coil of radius R_g begins to overlap with nearby coils, $c^* = M_w/(4/3)\pi R_g^3 N_A$,[37,38] where M_w is the molecular weight and N_A denotes Avogadro's number. From this we find that c^* is about 0.04 g/L based on an R_g of 0.7 μm for unstained λ-phage DNA obtained from New England BioLabs. (Similar estimates of R_g and of c^* can be obtained from recent work of Smith and coworkers,[39,40] who studied dsDNA molecules of several sizes, including one with around 7% fewer basepairs than λ-phage DNA, for which they estimated $c^* = 0.047$ mg/mL. When corrected for the modest difference in size, this value is roughly consistent with the value of $c^* = 0.04$ g/L taken here.) To examine the effect of intramolecular chain interactions on the transient dynamics for DNA molecules near a surface, we used five solutions with concentrations of unlabeled λ-phage DNA of 0.1c^*, 0.25c^*, 0.5c^*, 1.0c^*, and 3.0c^*, which correspond to concentrations of 0.004, 0.01, 0.02, 0.04, and 0.12 g/L, respectively. The viscosity of the solvent in the final solution was around 46.0 cP at 24 °C. To visualize DNA molecules without producing an overintensity of fluorescence, a low concentration of labeled λ-phage DNA was added to those DNA solutions. The concentrations of the labeled λ-phage DNA in the final solutions were around 60−65 pg/μL. Labeling was done with YOYO-1 dye (Molecular Probes) at a dye:base pair molar ratio of 1:10.[31] The labeled λ-phage DNA has a contour length $L = 19.0$ μm.[31]

To make the solutions, we first dissolved sucrose (Crystalline/Certified ACS, Fisher Chemical) at various concentrations into a pH 8.0 TE buffer consisting of 10 mM Tris-HCl, 2 mM EDTA, and 10 mM NaCl. Then using large-orifice pipet tips (Fisher), we added different desired volumes of unstained 0.5 g/L λ-phage DNA solution (New England BioLabs) into the above sucrose solutions and allowed the DNA molecules to diffuse for 1 week at room temperature in the dark. The labeled λ-phage DNA solution[31] was then mixed with β-mercaptoethanol (Sigma) and the above sucrose-DNA solutions at a volume ratio of 1:6:143 in a glass vial. In order to mix the solution uniformly and also prevent the breakage of DNA molecules, the glass vial covered with aluminum foil was rotated by hand very gently in 24 cycles. In each cycle, after a 1 min rotation, the solution relaxed in the dark for about 9 min, before the next rotation.

Experimental Setup. The torsional flow cell was mounted on the motorized stage of a Nikon TE200 fluorescence microscope, with the upper plate rotated by a motor, while the lower plate was a replaceable glass coverslip.[41,42] The alignment method was described by Li et al.[42] Detailed particle image velocimetry (PIV) measurements of the flow field were performed, and these confirmed that the desired simple shearing flow was generated by the flow cell.[41]

Determination of Shear Rate and Solution Viscosity. The Weissenberg number ($Wi = \dot{\gamma}\tau$, with $\dot{\gamma}$ the applied shear rate, and τ the polymer's longest relaxation time) is used to characterize the flow strength. In our torsional shear cell,[35] with a gap of $h_{gap} = 0.5$ mm and top-plate rotational speed $\omega = 0.0636$ rev/s, the shear rate at $r = 3.0$ mm from the axis of rotation is given as

$$\dot{\gamma} = \frac{2\pi\omega r}{h_{gap}} = 2.4\ \mathrm{s}^{-1} \tag{1}$$

By using an AR1000 controlled stress rheometer (TA Instruments), we measured the viscosity vs the shear rate for samples with different concentrations of unstained λ-phage DNA, shown in Figure 1. Because of the rheometer's limited measurement range, accurate viscosity data cannot be obtained at a shear rate lower than 1.0 s^{-1}, so that the data cannot be fit directly to the Carreau−Yasuda model to get the values of zero-shear viscosities. However, the data

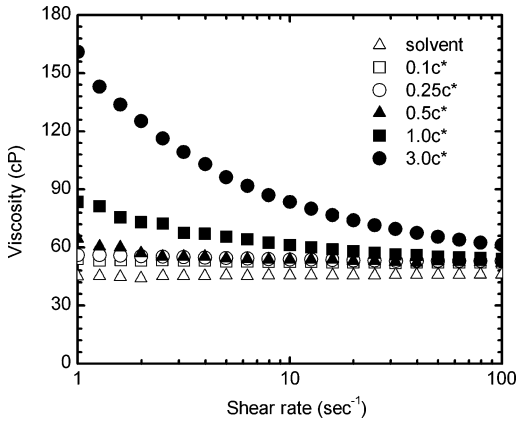

Figure 1. Viscosities of λ-phage DNA solutions with different concentrations vs shear rate at 24 °C.

Table 1. Lyons−Tobolsky Parameters for λ-Phage DNA Solutions and Zero-Shear Viscosities for Different DNA Concentrations

$[\eta]$ (L/g)	13.96				
k	0.54				
b (L/g)	−0.081				
c (g/L)	0.004	0.01	0.02	0.04	0.12
c/c^*	0.1	0.25	0.5	1.0	3.0
η_0 (cP)	48.6	52.9	60.9	80.7	235.4

in Figure 1 indicate that with an increased DNA concentration the zero-shear viscosity increases. Even at a concentration as low as 0.1c^*, the viscosity is higher than expected for dilute solutions due to interactions between polymer chains, which agrees with predictions of simulations.[26]

On the basis of the zero-shear viscosity data for λ-phage DNA in aqueous solutions without added sugar measured in a sensitive Contraves rheometer,[43] we can estimate the zero-shear viscosities for our DNA solutions by applying the Lyons−Tobolsky (LT) equation[44,45]

$$\frac{\eta_{sp}}{c[\eta]} = \exp\left\{\frac{k[\eta]c}{1 - bc}\right\} \tag{2}$$

where $\eta_{sp} = (\eta_0/\eta_s) - 1$, η_0 is the solution zero-shear viscosity, and η_s is the solvent viscosity; c is the concentration (expressed in units of mass of polymer per unit volume of solution); $[\eta]$ is the intrinsic viscosity of the polymer in the solvent in which η_0 is determined; k is the Huggins constant; and b is an empirical parameter. The zero-shear viscosity data of the sucrose-free λ-phage DNA aqueous solutions[43] were fit to the LT equation. The nonlinear least-squares fitting scheme provided in the OriginPro 7.5 (OriginLab Co.) was utilized to obtain the parameters, $[\eta]$, k, and b (shown in Table 1), and the R-square value is 0.985. Then we calculated the zero-shear viscosities for our λ-phage DNA solutions by retaining the same values of the above three parameters, while substituting the values of c and $\eta_s = 46.0$ cP for our experiments into the LT equation, giving the results in Table 1.

Image Acquisition and Analysis. We visualized stained DNA molecules in solution using the Nikon TE200 fluorescence microscope with a 100 × 1.3 objective, with a digital interline CCD camera CoolSNAP HQ (Roper Scientific) to capture images at a resolution of 1392 × 1040 pixels using full-chip acquisition. The image acquisition software MetaView/MetaMorph version 4.5 (Universal Image, distributed by Fryer Co.) was used to control the camera, the XYZ stage motor (Prior Inc.), and the electronic shutter (Uniblitz VMM-D1, Vincent Associates).

A 600 μL DNA solution was loaded into the shear cell using a large-orifice pipet tip (Fisher) to minimize damage to DNA molecules, and the top plate was lowered to 500 μm above the bottom surface using a micrometer. To block the evaporation from the solution, 100 μL of silicon oil was added to seal the gap between the shear head and the side wall of the cell. The solution was then allowed to relax for half an hour. To obtain the number density of

Table 2. Relaxation Time of λ-Phage DNA Molecules at Different Concentrations

c/c^*	0.1	0.25	0.5	1.0	3.0
η_0 (cP)	48.6	52.9	60.9	80.7	235.4
τ (s)	4.6	5.0	5.7	7.6	22.1

molecules in the bulk solution, 200 images with 40 ms exposure time were taken at different positions in the static solution at a distance of more than 35 μm above the bottom surface, which allowed the average number of molecules per frame to be determined to within 2.5%.

The stage was moved to the horizontal position (0, 3000 μm), where (0, 0) is the location of the rotation axis, and by focusing on marker particles[31] on the bottom surface, a reference vertical position ($H = 0$) for the stage was determined. Then the objective was raised to the desired vertical focal position ($H = 3$ μm). Rotation of the top plate began at time zero. To avoid artificially elongating the molecules due to image blurring under flow, the exposure time was limited to 40 ms at $H = 3$ μm. Under the torsional shearing flow, to make our experiments more efficient and also attain statistically accurate values of concentration and mean fractional stretch at each time point for a specific distance above the bottom surface, based on our experience, 100 images are needed, which require a time interval of 6.6 min.[31]

The offline software Metavue version 4.6r1 (Universal Imaging Corp.) was used to analyze the images. In our analysis, we included only molecules that were sharply focused, estimated from the experiments to be within ± 0.5 μm of the focal plane. The number of DNA molecules in each image was manually counted. The number density of DNA in the static solution was used as the original bulk concentration to normalize the number density of DNA in images acquired from each time period in the shear flow. Each reported mean fractional DNA stretch was obtained by averaging over more than 300 molecules and normalizing by the fully stretched length of the labeled λ-phage DNA, namely, $L = 19$ μm.

Results and Discussion

Hur et al.[38] found that in a shearing flow the rheological response of a semidilute DNA solution with DNA concentrations up to $6.0c^*$ is almost the same as in a dilute solution, but in a more viscous medium as a result of the increase in viscosity due to the surrounding chains. If we assume, as observed by Hur et al., that the relaxation time is proportional to the solution viscosity, then at increased DNA concentrations we can substitute the zero-shear viscosities η_0 in Table 1 into the known linear relationship between relaxation time and solvent viscosity[30] to calculate the relaxation time τ for λ-phage DNA molecules, given in Table 2.

To compare our experimental results with those in the very dilute regime, we used the same shear rate (2.4 s^{-1}) and solvent as in dilute solutions, but with increased DNA concentrations. The solvent viscosity is 46.0 cP; therefore, the relaxation time in dilute solution is 4.3 s,[32] and *Wi* based on this relaxation time is 10.3. Since the solution viscosity, and therefore the relaxation time, increases with concentration, the zero-shear *Wi* is higher than this, by up to a factor of 5 at $3.0c^*$. Since the solutions are highly shear thinning at high concentration, rather than attempt to correct the *Wi* for the effects of both concentration and shear thinning, here we characterize them by the nominal *Wi* based on the dilute-solution relaxation time.

The concentration profile in Figure 2 shows that for concentrations from $0.1c^*$ to $3.0c^*$ DNA molecules at 3 μm above the surface still migrate over time, although to a lesser extent than in dilute solution. At $3.0c^*$, the concentration of stained DNA at 3 μm from the surface at steady state is about 92% of the bulk value, compared to a relative concentration of 36% in very dilute solutions. The above results imply that the wall HI is weakened at higher DNA concentration due to the overlap of

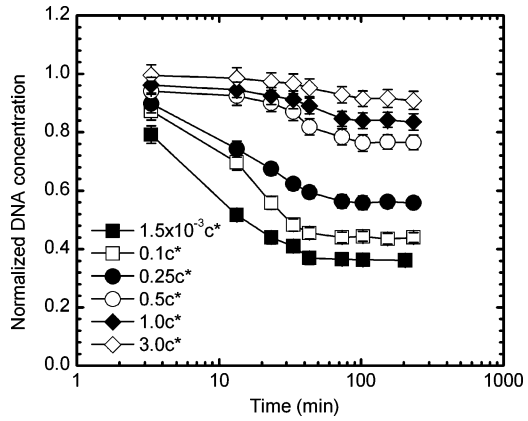

Figure 2. Normalized concentration against time for λ-phage DNA molecules in dilute and semidilute solutions at $H = 3$ μm (nominal $Wi = 10.3$). The error bars are standard errors.

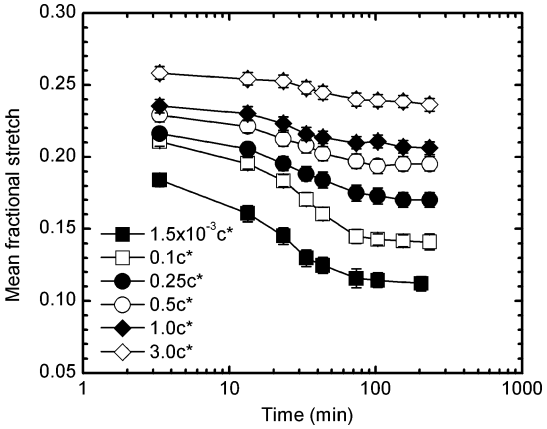

Figure 3. Same as in Figure 2, except for mean fractional stretch, rather than normalized DNA concentration.

polymer chains, and finally at $3.0c^*$, the wall HI is almost screened out, or at least that it no longer produces much diffusion away from the wall. The significant suppression of wall HI that we observe over the concentration range $0.1c^*$ to $1.0c^*$, along with simulation results indicating departure from dilute solution behavior both in the bulk[26] and near a wall[30] for polymer concentrations above $0.1c^*$ indicates that that both segment−segment and segment−wall HI start to become screened at concentrations above $0.1c^*$. This indicates that the Zimm model (for dominant HI in the bulk) begins to fail for concentrations as low as $0.1c^*$. In addition, in our simulations, for $c^* < c < 3.0c^*$, the existence of residual effects of HI implies that the overlapping chains may not follow Rouse-like behavior except in the range $3.0c^* < c < c_e$, where we can safely assume that the HI of the wall is thoroughly screened out.

The mean fractional stretch of DNA molecules near the surface shown in Figure 3 decreases over the same time scale over which migration occurs, which is probably due to the retention of some DNA fragments near the surface, as we inferred from results for dilute solutions.[31] At steady state, the mean fractional stretch of stained DNA molecules increases with concentration of unstained DNA molecules, which is probably caused by the suppression of migration of the longer chains and the increase of real *Wi* as a result of the increased solution viscosity.

Figures 2 and 3 reveal that increasing DNA concentration does not affect drastically the time scale for concentration and mean fractional stretch of DNA molecules near the surface to

reach steady state, which in fact only changes from 70 to 100 min. Our results suggest that the depletion-layer thickness L_d decreases up to 2−3-fold, owing to the screening of the HI by the overlap between polymer chains. However, the polymer diffusivity D decreases due to the increase of the solution viscosity, by up to a factor of 10 at a concentration of 6c*, according to recent data by Laib et al.[40] Since the time scale for the DNA concentration to reach steady state, t_s, should follow the scaling law $t_s \propto L_d^2/D$, we may infer that the reduced diffusion distance is roughly canceled out by the slower diffusion, resulting in little change in the diffusion time.

Conclusions

Fluorescence microscopic imaging of λ-phage DNA molecules was used to measure the time-dependent polymer concentration and mean fractional stretch near a nonadsorbing solid surface in a torsional shear flow for solutions with concentrations ranging from 0.1c* to 3.0c*. We focused on a nominal *Wi* of 10.3, based on the relaxation time of λ-phage DNA in dilute solution, which could be increased by a much as 5-fold if the *Wi* is instead based on the zero-shear semidilute relaxation time at 3.0c*. When the DNA concentration is less than 3.0c*, we find that the HI with the surface drives polymer chains away from the surface. This effect is weakened at higher DNA concentration due to the overlap of polymer chains, and finally at 3.0c*, the migration effect is almost screened out. From 0.1c* to 1.0c*, the significant suppression of the polymer migration that we observe, combined with Brownian dynamics simulations of polymers with HI in the bulk[26] and near a wall[30] indicate that both segment−segment and segment−wall HI begin to become screened at concentrations above 0.1c*. Hence, the Zimm model for dilute polymer chains in the bulk and related dilute-solution theory for polymers near surfaces is probably not appropriate for concentrations as low as 0.1c*. Although screening of HI begins at 0.1c*, even for $c^* < c < 3.0c^*$, we observe that the effects of the wall HI persist in attenuated form, implying that the overlapping chains may not reach the free-draining limit (i.e., Rouse behavior) until higher concentrations are achieved. For $3.0c^* < c < c_e$, the wall HI is almost totally screened out and the polymer chain behavior might obey the Rouse model, although at these concentrations the effects of occasional entanglements might be significant enough to invalidate the Rouse theory. Thus, both near a wall and possibly also in the bulk the polymer concentration regime between dilute and entangled may be better described as a broad crossover regime in which hydrodynamic interactions gradually fade out and entanglement effects emerge, rather than as a regime in which the Rouse model is valid.

Over the time scale for which polymer migration occurs, the mean fractional stretch of DNA molecules decreases, which is probably due to selective retention of fragments near the surface as long chains migrate away. The results also show that higher concentrations of DNA do not affect drastically the time scale for the DNA concentration and mean fractional stretch near the surface to reach steady state, which only changes from about 70 to 100 min. The similarity in time scales for diffusion in dilute and semidilute solutions is probably due to a cancellation of effects: the decreased depletion width at higher concentrations would accelerate the attainment of steady state were it not for the lower polymer diffusivity at these higher concentrations.

Acknowledgment. We thank NASA microgravity research division for supporting this study through Grant NAG3-2708.

References and Notes

(1) Graessley, W. W. *Polymer* **1980**, *21*, 258−262.
(2) de Gennes, P. G. *Scaling Concepts in Polymer Physics*; Cornell University Press: Ithaca, NY, 1979.
(3) Akcasu, A. Z.; Benmouna, M.; Han, C. C. *Polymer* **1980**, *21*, 866−890.
(4) Oono, Y. *Adv. Chem. Phys.* **1985**, *61*, 301−437.
(5) Doi, M. E.; Edwards, S. F. *The Theory of Polymer Dynamics*; Oxford Unversity Press: New York, 1986.
(6) Martin, J. E. *Macromolecules* **1986**, *19*, 1278−1281.
(7) Bhatt, M.; Jamieson, A. M.; Petschek, R. G. *Macromolecules* **1989**, *22*, 1374−1380.
(8) Pierleoni, C.; Ryckaert, J. P. *J. Chem. Phys.* **1992**, *96*, 8539−8551.
(9) Dünweg, B.; Kremer, K. *J. Chem. Phys.* **1993**, *99*, 6983−6997.
(10) Ahlrichs, P.; Dunweg, B. *J. Chem. Phys.* **1999**, *111*, 8225−8239.
(11) Freed, K. F.; Perico, A. *Macromolecules* **1981**, *14*, 1290−1298.
(12) Freed, K. F.; Edwards, S. F. *J. Chem. Phys.* **1974**, *61*, 3626−3633.
(13) de Gennes, P. G. *Macromolecules* **1976**, *9*, 594−598.
(14) Edwards, S. F.; Muthukumar, M. *Macromolecules* **1984**, *17*, 586−596.
(15) Richter, D.; Binder, K.; Ewen, B.; Stuhn, B. *J. Phys. Chem* **1984**, *88*, 6618−6633.
(16) Shiwa, Y.; Oono, Y.; Baldwin, P. R. *Macromolecules* **1988**, *21*, 208−214.
(17) Fredrickson, G. H.; Helfand, E. *J. Chem. Phys.* **1990**, *93*, 2048−2061.
(18) Colby, R. H.; Rubinstein, M.; Daoud, M. *J. Phys. II* **1994**, *4*, 1299−1310.
(19) Ahlrichs, P.; Everaers, R.; Dunweg, B. *Phys. Rev. E* **2001**, *6404*, 040501.
(20) Harnau, L. *J. Chem. Phys.* **2001**, *115*, 1943−1945.
(21) Ewen, B.; Richter, D. *Adv. Polym. Sci.* **1997**, *134*, 1−129.
(22) Kremer, K.; Grest, G. S. *J. Chem. Phys.* **1990**, *92*, 5057−5086.
(23) Rubinstein, M.; Colby, R. H. *Polymer Physics*; Oxford University Press: New York, 2003.
(24) Kaznessis, Y. N.; Hill, D. A.; Maginn, E. J. *J. Chem. Phys.* **1998**, *109*, 5078−5088.
(25) Ng, R. C. Y.; Leal, L. G. *J. Rheol.* **1993**, *37*, 443−468.
(26) Stoltz, C.; de Pablo, J. J.; Graham, M. D. *J. Rheol.* **2006**, *50*, 137−167.
(27) Ausserré, D.; Hervet, H.; Rondelez, F. *Macromolecules* **1986**, *19*, 85−88.
(28) Chauveteau, G.; Tirrell, M.; Omari, A. *J. Colloid Interface Sci.* **1984**, *100*, 41−54.
(29) Omari, A.; Moan, M.; Chauveteau, G. *Rheol. Acta* **1989**, *28*, 520−526.
(30) Hernández-Ortiz, J. P.; de Pablo, J. J.; Graham, M. D. *Phys. Rev. Lett.* **2007**, *98*, 140602.
(31) Fang, L.; Larson, R. G. *Macromolecules*, in press.
(32) Fang, L.; Hu, H.; Larson, R. G. *J. Rheol.* **2005**, *49*, 127−138.
(33) Jendrejack, R. M.; Dimalanta, E. T.; Schwartz, D. C.; Graham, M. D.; de Pablo, J. J. *Phys. Rev. Lett.* **2003**, *91*, 038102.
(34) Jendrejack, R. M.; Schwartz, D. C.; de Pablo, J. J.; Graham, M. D. *J. Chem. Phys.* **2004**, *120*, 2513−2529.
(35) Ma, H. B.; Graham, M. D. *Phys. Fluids* **2005**, *17*, 083103.
(36) Chen, Y. L.; Graham, M. D.; de Pablo, J. J.; Jo, K.; Schwartz, D. C. *Macromolecules* **2005**, *38*, 6680−6687.
(37) Larson, R. G. *The Structure and Rheology of Complex Fluids*; Oxford University Press: New York, 1999.
(38) Hur, J. S.; Shaqfeh, E. S. G.; Babcock, H. P.; Smith, D. E.; Chu, S. *J. Rheol.* **2001**, *45*, 421−450.
(39) Roberson, R. M.; Laib, S.; Smith, D. E. *Proc. Natl. Acad. Sci. U.S.A.* **2006**, *103*, 7310−7314.
(40) Laib, L.; Robertson, R. M.; Smith, D. E. *Macromolecules* **2006**, *39*, 4114−4119.
(41) Hu, H.; Larson, R. G.; Magda, J. J. *J. Rheol.* **2002**, *46*, 1001−1021.
(42) Li, L.; Hu, H.; Larson, R. G. *Rheol. Acta* **2004**, *44*, 38−46.
(43) Heo, Y.; Larson, R. G. *J. Rheol.* **2005**, *49*, 1117−1128.
(44) Lyons, P. F.; Tobolsky, A. V. *Polym. Eng. Sci.* **1970**, *10*, 1−3.
(45) Rink, M.; Pavan, A.; Roccasalvo, S. *Polym. Eng. Sci.* **1978**, *18*, 755−766.

MA0626315